HEP'99 # 6_362
Submitted to Pa 6, 7
Pl 6, 7

DELPHI 99-135 CONF 322
15 June 1999

Results on Fermion-Pair Production at LEP running near 183 and 189 GeV

Preliminary

DELPHI Collaboration

Paper submitted to the HEP'99 Conference
Tampere, Finland, July 15-21

DELPHI 99-135 CONF 322

Results on Fermion-Pair Production at LEP running near 183 and 189 GeV

Preliminary

DELPHI Collaboration

A.Behrmann[1], I.Boyko[2], T.Burgsmüller[1], M.Calvi[3], P.Checchia[4], G.Della Ricca[5], D.Gelé[6], J.Holt[8], J.Libby[8], M.Nikolenko[2], A.Olchevski[2], M.Paganoni[9], D.Reid[9], P.Renton[8], T.Myklebust[10], G.Morton[8], F.Terranova[9], G.R.Wilkinson[8], M.Winter[6], V.Zhuravlov[2]

Abstract

A preliminary analysis of the data collected in 1997 and 1998 with the DELPHI detector at e^+e^- collision energies close to 183 and 189 GeV was performed in order to extract the hadronic and leptonic cross-sections, as well as the leptonic forward-backward asymmetries. Various interpretations of the results, including possible physics beyond the Standard Model, are presented. In particular, the data are used to investigate potential contact interactions, R-parity violating SUSY particles and Z' bosons and gravity in extra dimensions.

Paper prepared for summer conferences 1999

[1]Fachbereich Physik, University of Wuppertal, Wuppertal, FRG
[2]Joint Institute for Nuclear Research, Dubna, Russia
[3]INFN, Milano, Italy
[4]INFN, Padova, Italy
[5]INFN, Trieste, Italy
[6]Institut de Recherches Subatomiques, IN2P3-CNRS/ULP, Strasbourg, France
[7]INFN, Torino, Italy
[8]Department of Physics, University of Oxford, Oxford,UK
[9]European Laboratory for Particle Physics (CERN), Geneva, Switzerland
[10]University of Oslo, Institute of Physics, Oslo, Norway

1 Introduction

Preliminary results are presented from the analyses of fermion-pair final states collected in 1997 and 1998 with the DELPHI experiment at a mean centre–of–mass energy of about 183 and 189 GeV. These results complement those obtained from 1995 to 1997 [1], at lower collision energies ($130 - 172$ GeV). complement those obtained from 1995 to 1997 [1], at lower collision energies ($130 - 172$ GeV).

In the present paper inclusive hadronic, electron-pair, muon-pair and tau-pair final states are analysed. Measurements of the cross sections and leptonic forward–backward asymmetries for these final states at $\sqrt{s} \sim 189$ GeV, together with the ones presented in [1] and from LEP running in the vicinity of the Z-resonance [2, 3], are used to update the results of [1] and where fits which included physics beyond the Standard Model were performed. Signs of new physics are investigated here in terms of contact interactions, R-parity violating SUSY, additionnal neutral gauge bosons and gravity in extra dimension. For the theoretical motivation and technical details the reader is referred to [1].

2 Measurements of cross-sections and asymmetries

The luminosity analysis of the data collected during LEP operation in 1998 follows closely the one described in [1]. The total experimental systematic uncertainty on the integrated luminosity determination amounts to 0.50%, to combine with a 0.25% uncertainty reflecting the precision of the theoretical calculations underlying the computation of the visible cross-section of the luminometers.

An estimate of the mean centre–of–mass energy led to values of (182.70 ± 0.05) and (188.70 ± 0.05) GeV.

The results on the cross section and leptonic forward–backward asymmetry measurements presented in this section are from the analyses of e^+e^-, $\mu^+\mu^-$, $\tau^+\tau^-$ and inclusive hadronic final states. These analyses were similar to the ones performed at lower energies and the details, such as event selection, reduced energy ($\sqrt{\mathrm{s}'}$) determination can be found in [1]. The distributions of $\sqrt{\mathrm{s}'}/\sqrt{\mathrm{s}}$ obtained for the real and the simulated data are shown in Figure 1 for the hadronic channel and 2 for the muon and tau channels.

Systematic uncertainties associated with the cross section and asymmetry analyses for the different final states and $\sqrt{\mathrm{s}'}$ ranges are provided in Table 1.

The luminosity and statistics accumulated at centre-of-mass energies near 183 and 189 GeV are summarised in Table 2 for the inclusive $e^+e^- \rightarrow q\bar{q}(\gamma)$ and leptonic final states. The results of the cross-section and asymmetry measurements are presented in Table 3. The errors indicated are statistical only. Systematic errors due to the event selection and to the residual background subtraction are shown in Table 1. They are to be added in quadrature to the systematic uncertainty coming from the luminosity determination.

Figures 3 and 4 show the measured hadron, muon-pair and tau-pair cross-sections and forward–backward asymmetries, for all collision energies ranging from the Z^0-peak up to 189 GeV. The curves show the ZFITTER predictions. Equivalent plots for electrons are given in figures 5 and 6.

Overall, no substantial departure of the measurements from the theoretical predictions was found.

	$\sqrt{s}$ GeV	$\Delta\sigma^h/\sigma^h$ %	$\Delta\sigma^\mu/\sigma^\mu$ %	$\Delta\sigma^\tau/\sigma^\tau$ %	ΔA^μ_{FB} 10^{-3}	ΔA^τ_{FB} 10^{-3}
$\sqrt{s'}/\sqrt{s} > 0.85$	183	3.0	2.5	3.0	15	30
	189	1.8	3.8	4.0	20	15
"Total"	183	1.1	2.5	3.0	10	30
	189	1.1	3.3	6.0	20	15

Table 1: Systematic uncertainties of the total and non-radiative cross section and forward–backward asymmetry measurements for the three final states. "Total" refers to $\sqrt{s'}/\sqrt{s} > 0.10$ for the hadronic final states and to $\sqrt{s'} > 75$ GeV for the leptonic ones.

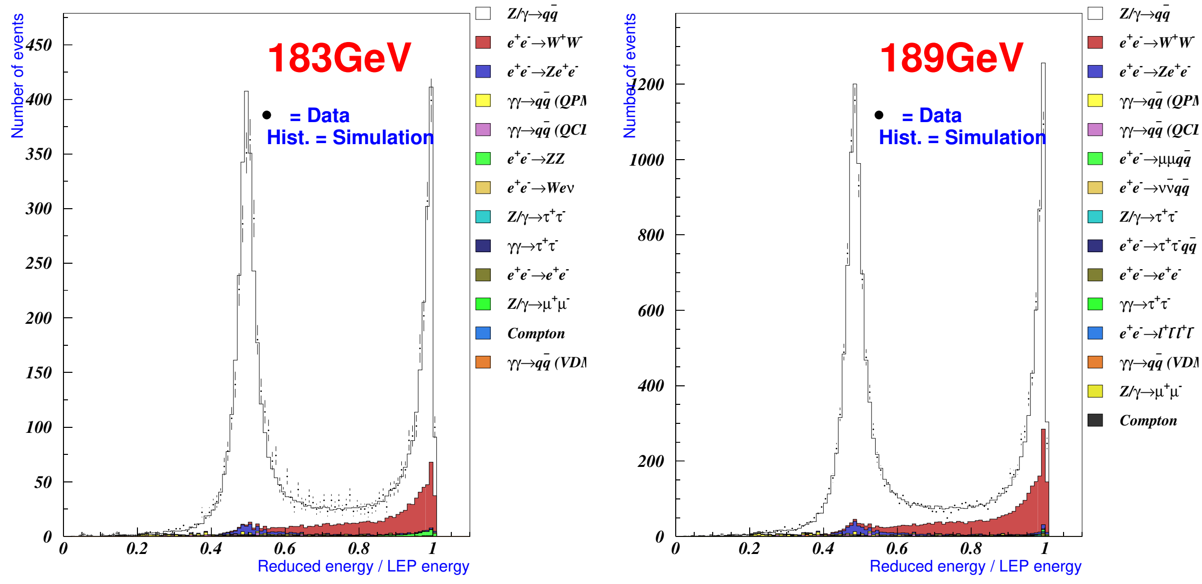

Figure 1: Distribution of the reconstructed reduced energy for the $e^+e^- \to q\bar{q}(\gamma)$ process at $\sqrt{s} \sim 183$ and 189 GeV. The points show the real data and the histogram stands for the simulated signal and background samples.

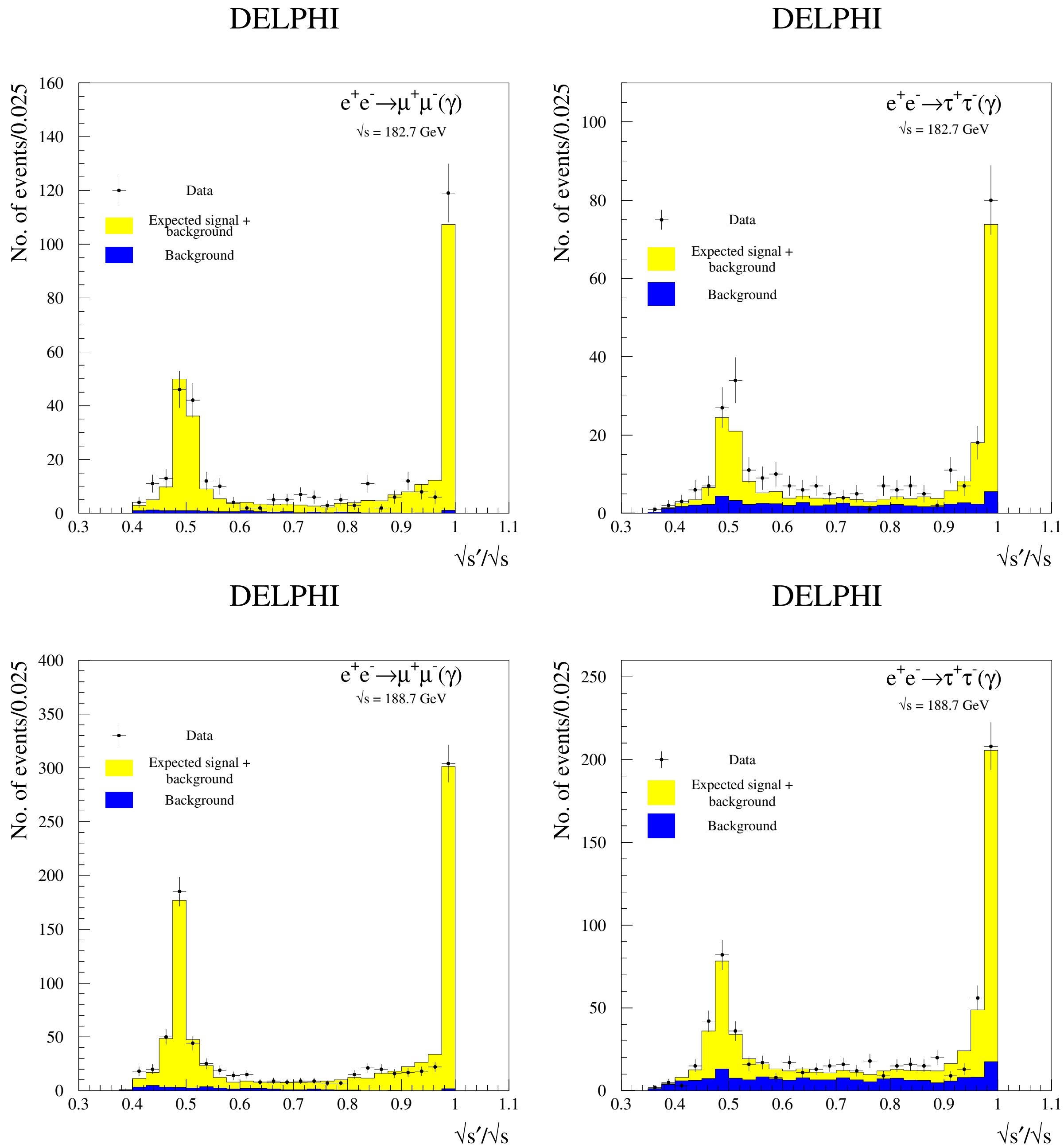

Figure 2: Distribution of the reconstructed reduced energy for the $e^+e^- \rightarrow \mu^+\mu^-(\gamma)$ and $e^+e^- \rightarrow \tau^+\tau^-(\gamma)$ processes at $\sqrt{s} \sim 183$ and 189 GeV. The points stand for the data and the histogram represents the sample simulated with the KORALZ generator normalised to the ZFITTER predictions.

Energy (GeV)		182.7	188.7
Integrated Luminosity (pb^{-1})		53.5	155.2
Number of events:	$e^+e^- \to q\bar{q}(\gamma)$	6024	15725
	$e^+e^- \to e^+e^-(\gamma)$	1109	2804
	$e^+e^- \to \mu^+\mu^-(\gamma)$	354	880
	$e^+e^- \to \tau^+\tau^-(\gamma)$	232	682

Table 2: Integrated luminosity and statistics used in the analyses of the different final states. For each channel, the values refer to the samples with $\sqrt{\mathrm{s}'/s} > 0.10$ for hadrons, $\sqrt{\mathrm{s}'} > 0.75$ for muons and taus and $\theta_{acol} < 20°$for electrons.

Energy (GeV)		182.7	188.7
$\sigma_{had}(pb)$	$\sqrt{\mathrm{s}'}/\sqrt{\mathrm{s}} > 0.85$	26.8 ± 0.8	22.1 ± 0.5
	$\sqrt{\mathrm{s}'}/\sqrt{\mathrm{s}} > 0.10$	110.3 ± 1.7	97.1 ± 1.0
$\sigma_{\mu\mu}(pb)$	$\sqrt{\mathrm{s}'}/\sqrt{\mathrm{s}} > 0.85$	3.54 ± 0.28	3.02 ± 0.15
	$\sqrt{s'} > 75$ GeV	8.83 ± 0.47	7.27 ± 0.24
$\sigma_{\tau\tau}(pb)$	$\sqrt{\mathrm{s}'}/\sqrt{\mathrm{s}} > 0.85$	3.59 ± 0.42	3.22 ± 0.23
	$\sqrt{s'} > 75$ GeV	8.65 ± 0.80	7.47 ± 0.39
$\mathrm{A}^{\mu}_{\mathrm{FB}}$	$\sqrt{\mathrm{s}'}/\sqrt{\mathrm{s}} > 0.85$	0.562 ± 0.067	0.582 ± 0.041
	$\sqrt{s'} > 75$ GeV	0.288 ± 0.051	0.362 ± 0.032
$\mathrm{A}^{\tau}_{\mathrm{FB}}$	$\sqrt{\mathrm{s}'}/\sqrt{\mathrm{s}} > 0.85$	0.678 ± 0.085	0.683 ± 0.051
	$\sqrt{s'} > 75$ GeV	0.399 ± 0.086	0.425 ± 0.049
$\sigma_{ee}(pb)$	$\theta_{acol} < 20°$	25.6 ± 0.8	22.8 ± 0.4
$\mathrm{A}^{e}_{\mathrm{FB}}$	$\theta_{acol} < 20°$	0.814 ± 0.017	0.812 ± 0.011

Table 3: Results of the cross-section and asymmetry measurements for the different final states. The errors indicated are statistical only. Systematic errors related to the event selection and residual backgrounds are provided in Table 1. Those coming from the luminosity determination are given in the text. The hadronic, muon and tau results are corrected for all cuts, apart from the $\sqrt{s'}$ cut.

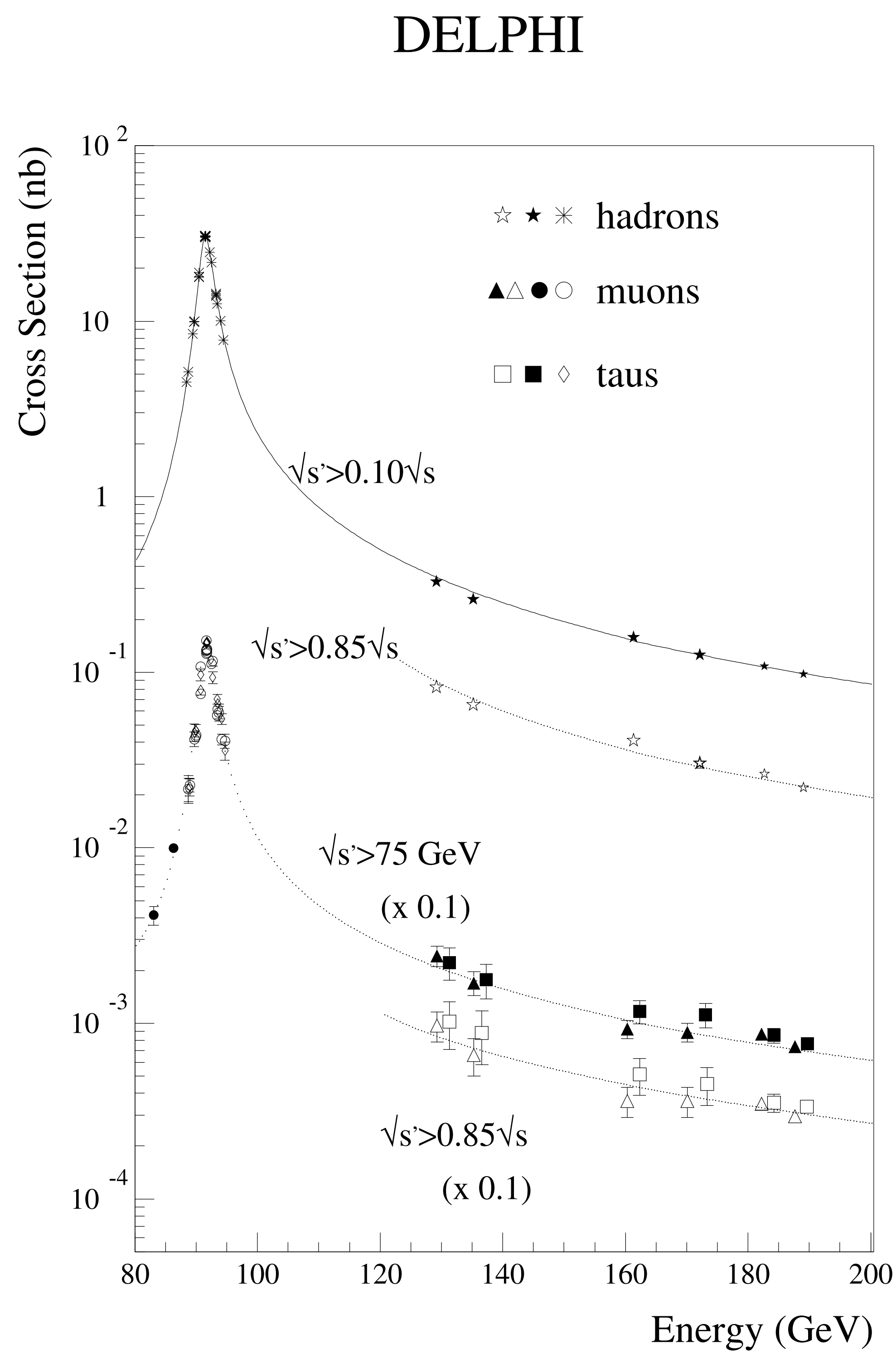

Figure 3: Cross-sections for the $e^+e^- \to q\bar{q}(\gamma)$, $\mu^+\mu^-(\gamma)$ and $\tau^+\tau^-(\gamma)$ processes measured at energies near the Z^0-resonance peak up to 189 GeV. The data at the Z resonance are the published results of the Z lineshape corrected to the acceptance $\sqrt{s'} > 0.1\sqrt{s}$ for hadrons and $\sqrt{s'} > 75$ GeV for leptons. The curves are the predictions of the ZFITTER program.

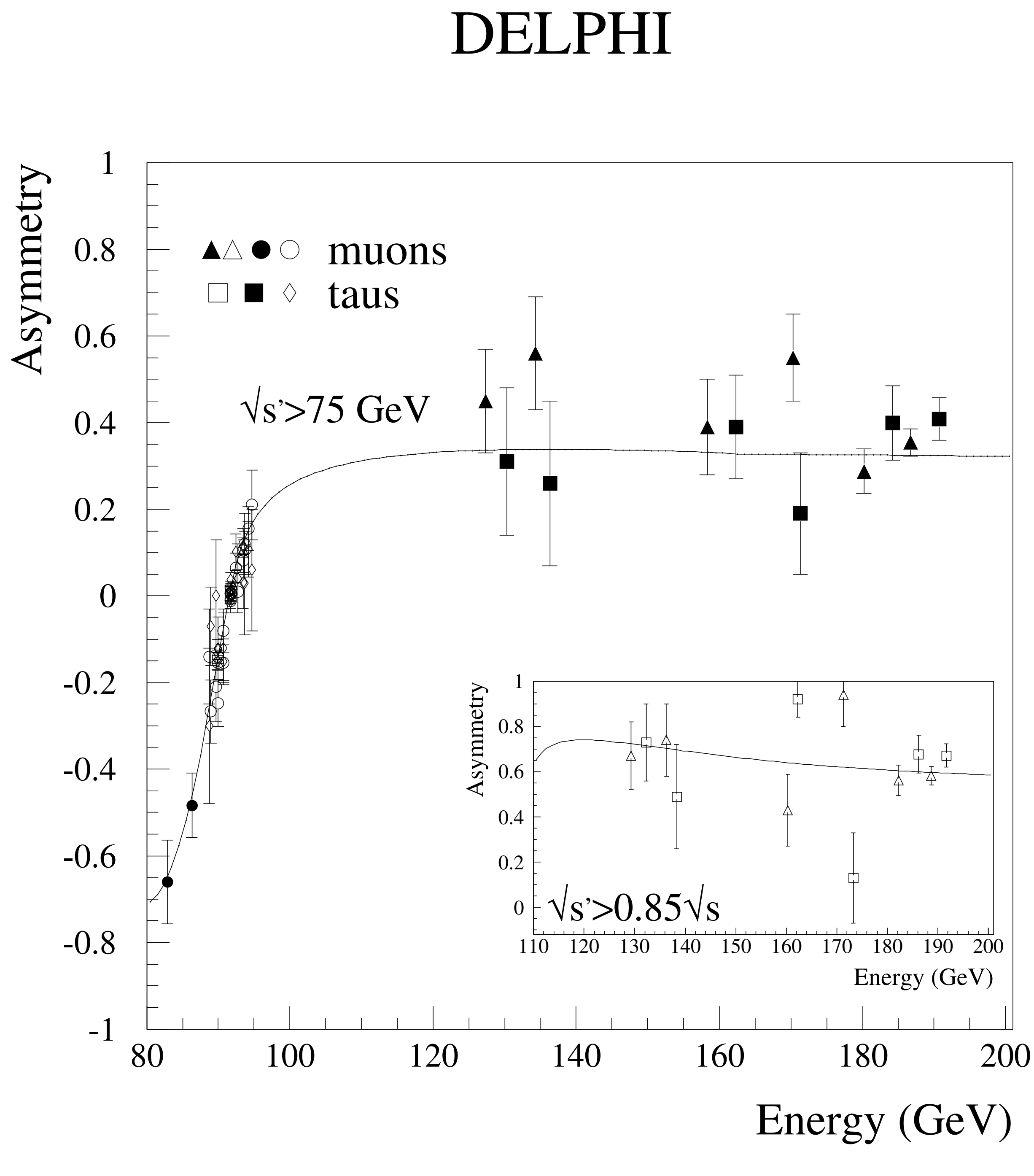

Figure 4: The forward–backward charge asymmetries in the reactions $e^+e^- \rightarrow \mu^+\mu^-(\gamma)$ and $\tau^+\tau^-(\gamma)$ measured at energies ranging from the Z^0-peak vicinity up to 189 GeV. The data at the Z resonance are the published results from Z-resonance running corrected to the acceptance $\sqrt{s'} > 75$ GeV. The curves are the predictions of the ZFITTER program.

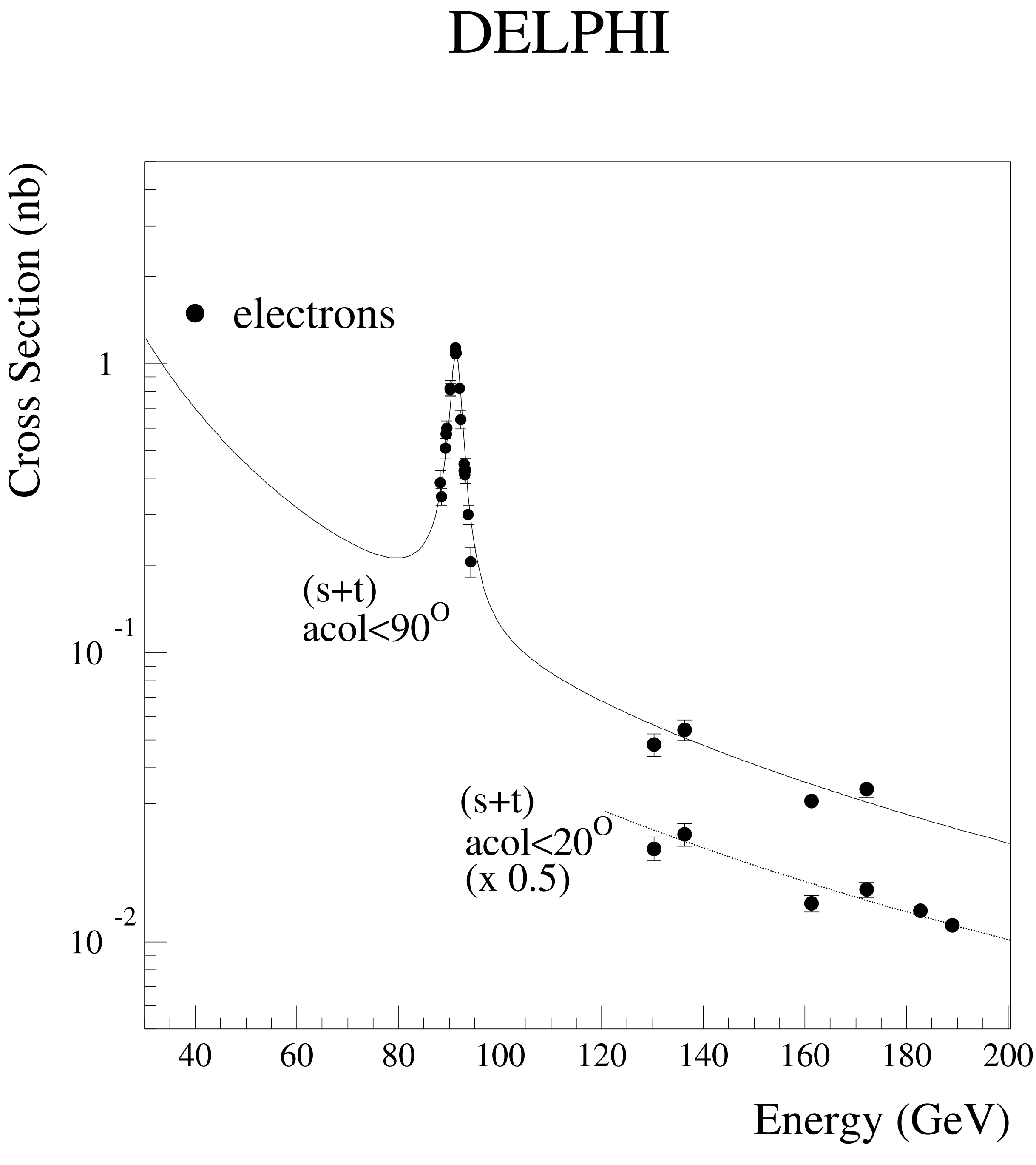

Figure 5: Cross-sections for the $e^+e^- \rightarrow e^+e^-(\gamma)$ process measured at energies near the Z^0-resonance peak up to 189 GeV. The curves are the predictions of the TOPAZ0 program.

DELPHI

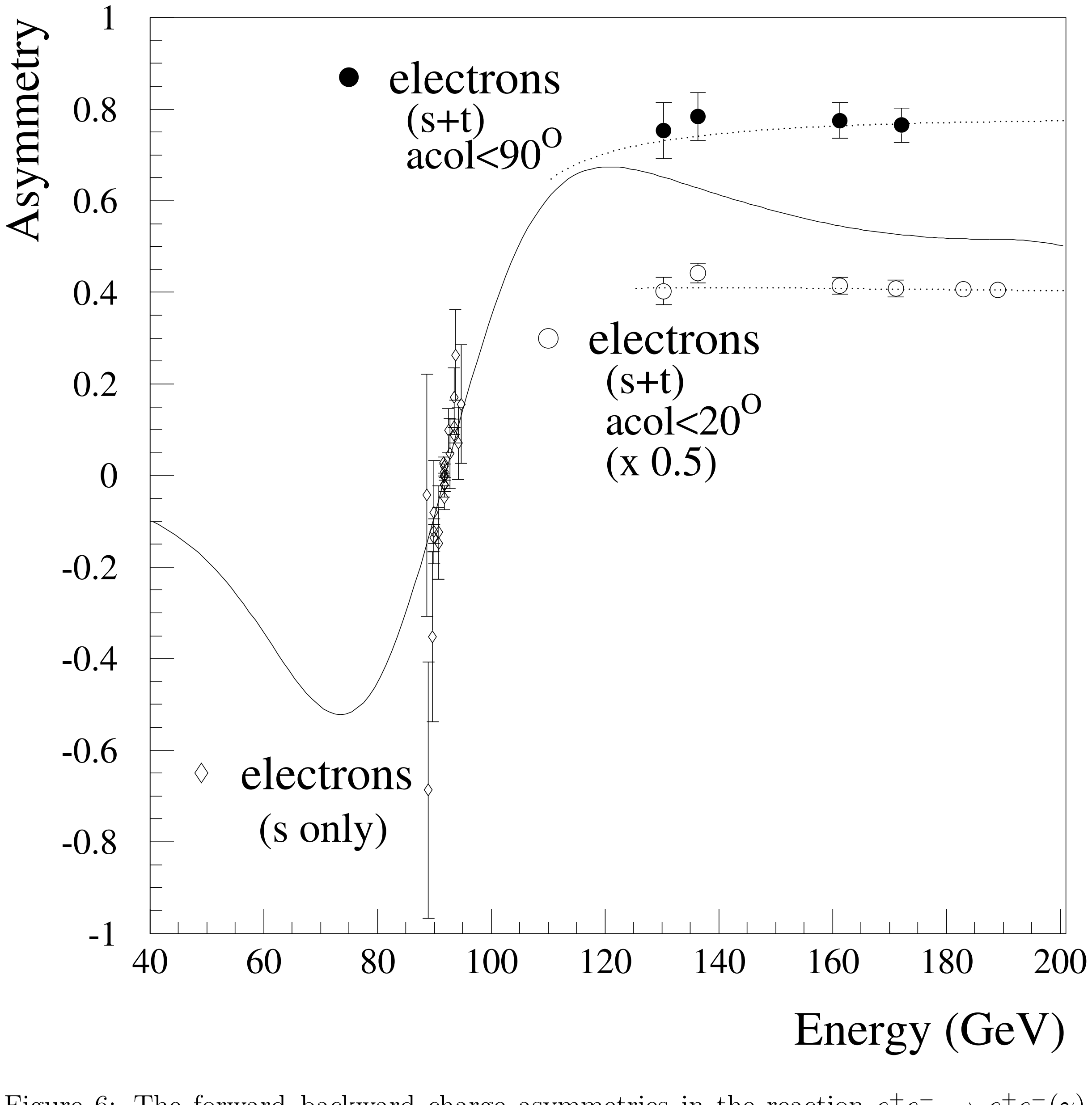

Figure 6: The forward–backward charge asymmetries in the reaction $e^+e^- \to e^+e^-(\gamma)$ measured at energies ranging from the Z^0-peak vicinity up to 189 GeV. The curves are the predictions of the TOPAZ0 program.

3 Fits to physics beyond the Standard Model

The data presented in this paper were used to improve the constraints on physics beyond the Standard Model obtained in [1]. A variety of models are discussed in section 5 of [1]. Updates to the results presented in section 6 of [1] are given below for three sets of models: contact interactions between leptons, models including Z′ bosons and sneutrino exchange. New limts are given for models which include gravity in extra dimensions.

3.1 Contact interaction models

The parameter fitted is $\epsilon = 1/\Lambda^2$, where Λ is the scale of the interactions in the effective Lagrangian of the four-fermion interactions

$$\mathcal{L}_{eff} = \frac{g^2}{(1+\delta)\Lambda^2} \sum_{i,j=L,R} \eta_{ij} \overline{e}_i \gamma_\mu e_i \overline{f}_j \gamma^\mu f_j, \tag{1}$$

see sections 5.1 and 6.1.1 of [1] for more details.

Fits were made for all channels using data at all energies from 130 to 189 GeV. The values of ϵ extracted for each model were all compatible with the Standard Model expectation $\epsilon = 0$, at the two standard deviation level. The errors on ϵ in the $e^+e^- \to l^+l^-$ fit are typically 30% of those reported in [1] as a result of the inclusion of the data collected at $\sqrt{s} \sim 183$ and 189 GeV. The fitted values of ϵ were converted into lower limits on Λ at 95% confidence level. The results are given in Table 4, and the 95% confidence bands of ϵ are shown in Figure 7.

3.2 Sneutrino exchange

The second set of models consider possible s or t channel sneutrino ($\tilde{\nu_\ell}$) exchange in R-parity violating supersymmetry. The purely leptonic part of the R-parity violating superpotential has the form

$$\lambda_{ijk} L^i_L L^j_L \overline{E}^k_R$$

The parameters of interest are the coupling λ_{ijk} and the mass of the sneutrino exchanged, $m_{\tilde{\nu}}$. The sneutrino width is not constrained within R-parity violating supersymmetry. A value of 1 GeV has been used [4]. Further details can be found in sections 5.2 and 6.1.2 of [1].

For the $e^+e^- \to \mu^+\mu^-$ and $e^+e^- \to \tau^+\tau^-$ channels, in the case that only one λ value is non-zero there are only t-channel sneutrino effects. Assuming sneutrino masses of 100 and 200 GeV. The values of λ obtained for the $e^+e^- \to \mu^+\mu^-$ and $e^+e^- \to \tau^+\tau^-$ channels are all consistent with zero, translating into the 95% confidence exclusion limits provided in Table 5.

Fits for the $e^+e^- \to e^+e^-$ channel the resulting 95% limits on λ, are given in Figure 8(a), as a function of $m_{\tilde{\nu}}$. For the fits in the $e^+e^- \to \mu^+\mu^-$ channel, assuming that $\lambda_{131} = \lambda_{232} = \lambda$, the resulting 95% limits on λ are given in Figure 8(b). The exclusion contour for $\lambda_{121} = \lambda_{233} = \lambda$, using the $e^+e^- \to \tau^+\tau^-$ channel, is shown in Figure 8(c). A coupling of $\lambda > 0.1$ can be excluded for $m_{\tilde{\nu}}$ in the range 130 - 190 GeV for all final states.

$e^+e^- \to e^+e^-$			
Model	$\epsilon^{+\sigma_+}_{-\sigma_-}$ (TeV^{-2})	Λ^+(TeV)	Λ^-(TeV)
LL	$0.011^{+0.017}_{-0.020}$	5.1	5.8
RR	$0.007^{+0.021}_{-0.016}$	4.9	5.7
VV	$0.000^{+0.004}_{-0.003}$	12.1	12.7
AA	$0.011^{+0.007}_{-0.011}$	6.7	8.2
RL	$-0.005^{+0.015}_{-0.010}$	7.0	6.8
LR	$-0.005^{+0.015}_{-0.010}$	7.0	6.8

$e^+e^- \to \mu^+\mu^-$			
Model	$\epsilon^{+\sigma_+}_{-\sigma_-}$ (TeV^{-2})	Λ^+(TeV)	Λ^-(TeV)
LL	$-0.002^{+0.015}_{-0.015}$	6.4	6.1
RR	$-0.002^{+0.016}_{-0.017}$	6.1	5.8
VV	$0.001^{+0.004}_{-0.007}$	10.4	9.7
AA	$0.001^{+0.006}_{-0.009}$	8.9	8.3
RL	$-0.246^{+0.265}_{-0.034}$	2.0	1.8
LR	$-0.246^{+0.265}_{-0.034}$	2.0	1.8

$e^+e^- \to \tau^+\tau^-$			
Model	$\epsilon^{+\sigma_+}_{-\sigma_-}$ (TeV^{-2})	Λ^+(TeV)	Λ^-(TeV)
LL	$0.011^{+0.021}_{-0.020}$	4.6	5.4
RR	$0.014^{+0.022}_{-0.023}$	4.5	5.2
VV	$-0.003^{+0.006}_{-0.009}$	8.9	7.4
AA	$0.019^{+0.011}_{-0.009}$	5.1	7.7
RL	$-0.175^{+0.137}_{-0.047}$	2.6	2.0
LR	$-0.175^{+0.137}_{-0.047}$	2.6	2.0

$e^+e^- \to l^+l^-$			
Model	$\epsilon^{+\sigma_+}_{-\sigma_-}$ (TeV^{-2})	Λ^+(TeV)	Λ^-(TeV)
LL	$0.003^{+0.011}_{-0.009}$	6.8	7.8
RR	$0.007^{+0.009}_{-0.012}$	6.8	7.6
VV	$0.001^{+0.001}_{-0.004}$	14.7	12.7
AA	$0.008^{+0.004}_{-0.006}$	8.0	10.9
RL	$-0.011^{+0.012}_{-0.008}$	7.8	6.4
LR	$-0.011^{+0.012}_{-0.008}$	7.8	6.4

Table 4: Fitted values of ϵ and 95% confidence limits on the scale, Λ, of contact interactions in the models discussed in the text, for $e^+e^- \to e^+e^-$, $e^+e^-\to\mu^+\mu^-$, $e^+e^-\to\tau^+\tau^-$ and also for $e^+e^- \to l^+l^-$ in which lepton universality is assumed for the contact interactions. The errors on ϵ are statistical only.

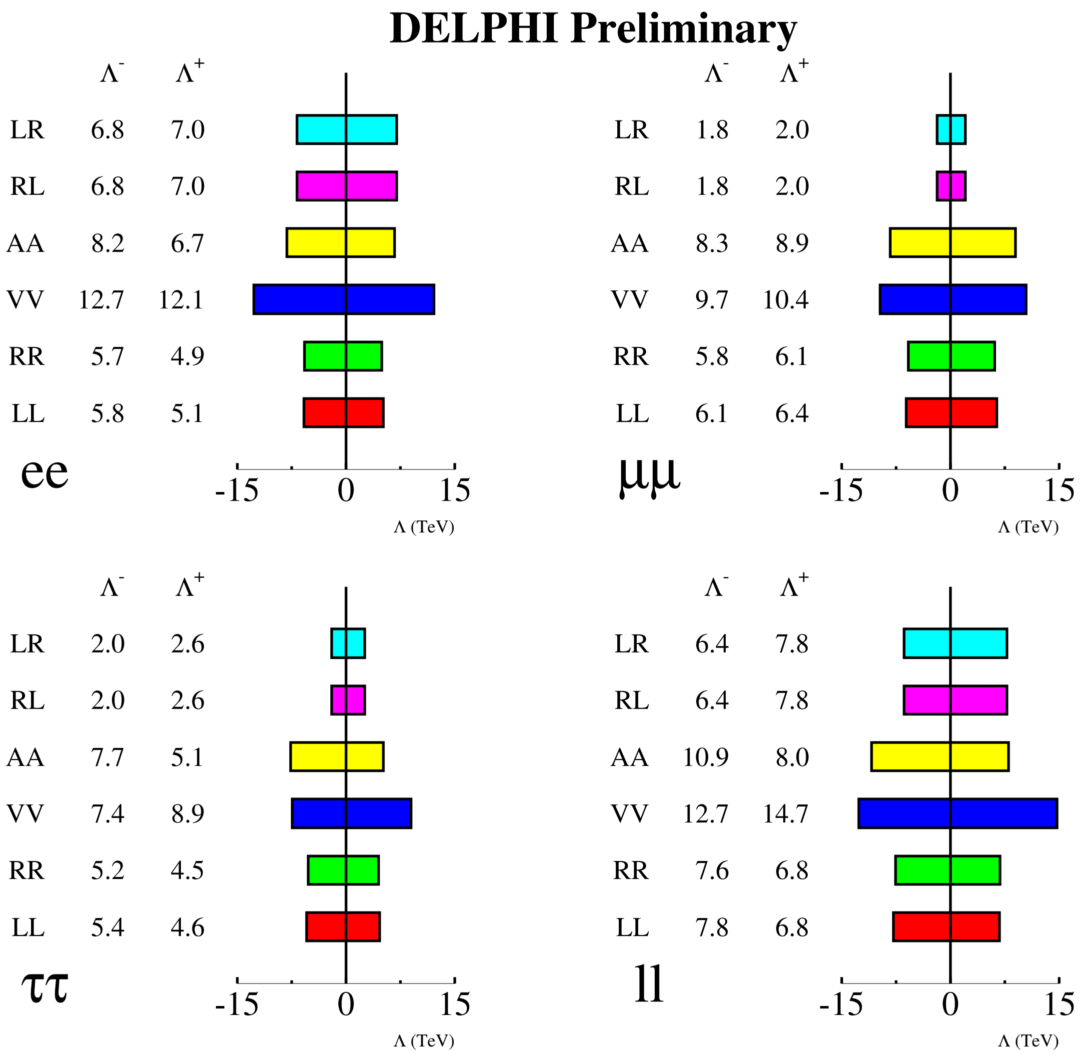

Figure 7: The 95% confidence allowed limits of ϵ for $e^+e^- \to e^+e^-$, $e^+e^- \to \mu^+\mu^-$, $e^+e^- \to \tau^+\tau^-$ and $e^+e^- \to l^+l^-$ in different helicity models of contact interactions. The results for $e^+e^- \to e^+e^-$ include data from 130-172 only. All other channels contain also data collected near 183 and 189 GeV.

coupling	$m_{\tilde{\nu}} = 100$ GeV/c^2 (95% c.l.)	$m_{\tilde{\nu}} = 200$ GeV/c^2 (95% c.l.)
λ (t-chann. $\tilde{\nu}_\ell$ in $e^+e^- \to \mu^+\mu^-$)	0.50	0.69
λ (t-chann. $\tilde{\nu}_\ell$ in $e^+e^- \to \tau^+\tau^-$)	0.49	0.67

Table 5: Limits on the couplings λ in t channel sneutrino exchange in $e^+e^- \to \mu^+\mu^-$ and $e^+e^- \to \tau^+\tau^-$ for sneutino massesof 100 and 200 GeV. The couplings involved are given in the text.

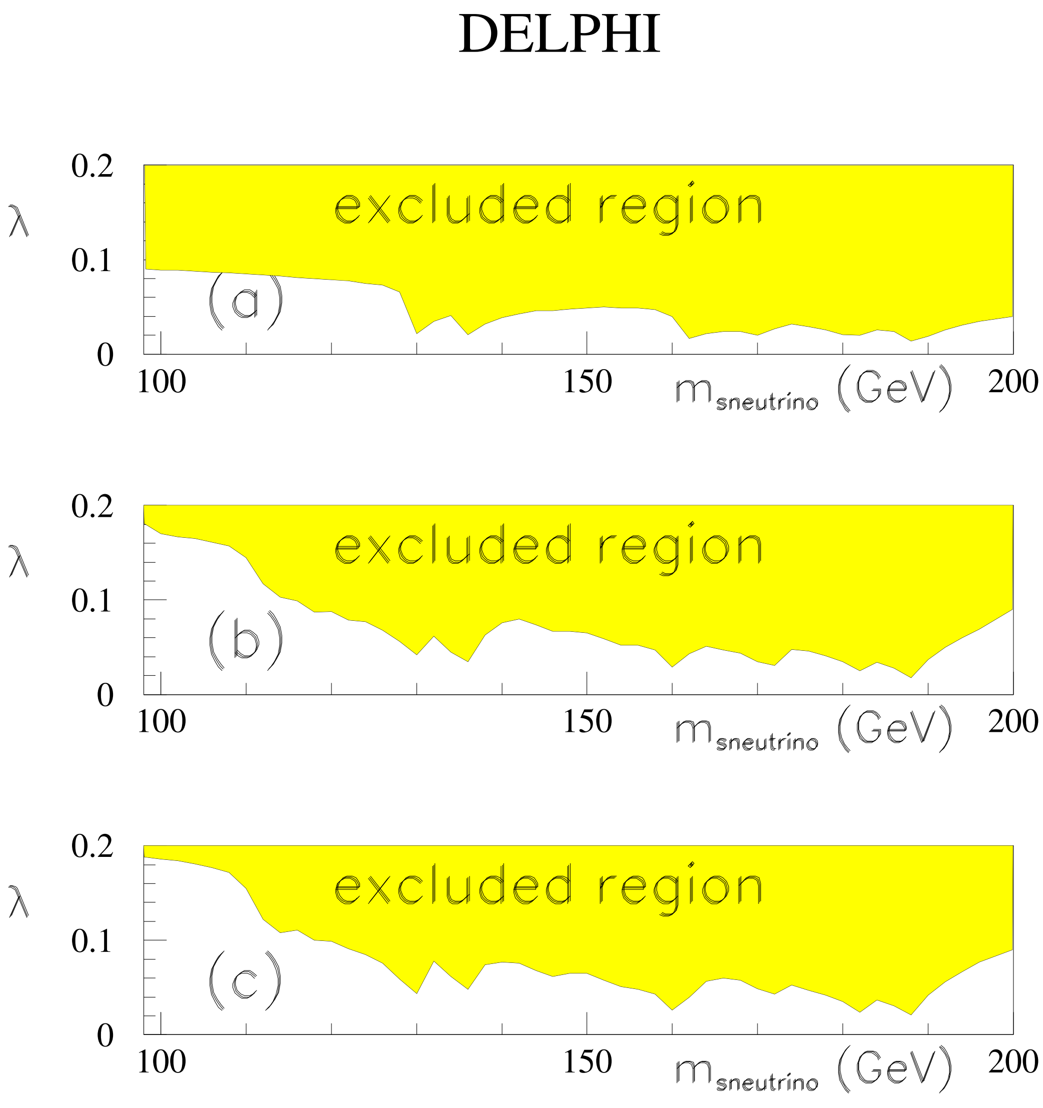

Figure 8: The 95% exclusion limits for (a) λ_{121} (or λ_{131}), as a function of $m_{\tilde{\nu}}$ obtained from the $e^+e^- \to e^+e^-$ channel; (b) $\lambda_{131} = \lambda_{232} = \lambda$, as a function of $m_{\tilde{\nu}}$ obtained from the $e^+e^- \to \mu^+\mu^-$ channel; (c) $\lambda_{121} = \lambda_{233} = \lambda$, as a function of $m_{\tilde{\nu}}$ obtained from the $e^+e^- \to \tau^+\tau^-$ channel. The sneutrino width is taken to be 1 GeV.

Model	χ	ψ	η	L-R
$M_{\mathrm{Z}'}^{limit}$	430 GeV	345 GeV	305 GeV	370 GeV
$\mid \theta_{ZZ'}^{limit} \mid$	0.0017	0.0018	0.0025	.0019

Table 6: 95% confidence level lower limits on the Z' mass and upper limits on the ZZ' mixing angle within the χ, ψ, η and L-R models.

3.3 Z'-bosons

Existing data from LEP1 and LEP2 and the cross-sections and asymmetries given here were used to fit the data to models including additional Z' bosons.

Fits were made to the mass of a Z' and of the Z, and to the mixing angle between the two bosonic fields. More details can be found in section 5.4.1 and 6.3.1 of [1]. The fitted Z-mass was found in agreement with its standard value. No evidence was found for the existence of a Z'-boson in any of the models. The 95 % confidence level limits on $M_{\mathrm{Z}'}$ and $\theta_{ZZ'}$ were computed for each model by determining the contours of the domain in the $M_{\mathrm{Z}'} - \theta_{ZZ'}$ plane where $\chi^2 < \chi^2_{min} + 5.99$. The allowed regions for $M_{\mathrm{Z}'}$ and $\theta_{ZZ'}$ are shown in Figure 9, where the contours obtained in [1] are shown for comparison. The lower limits on the Z' mass found in [1], which range from 305 to 430 GeV, improve by 105 – 180 GeV depending on the model.

3.3.1 Model independent fits

Fits were performed to the leptonic cross-sections and forward-backward asymmetries, for the leptonic coupling of a Z', $a_{l'}^N$ and $v_{l'}^N$ normalised for the overall coupling scale and the mass of the Z'. See section 5.4.2 and 6.3.2 of [1] for more details.

Several values of the mass of the Z' were considered (i.e. 300, 500 and 1000 GeV), and the ZZ'-mixing was neglected. Figure 10 shows the values of the couplings a'_f and v'_f which are compatible with the DELPHI data with a confidence level of 95%. The limits on the normalised couplings found in [1], i.e. $|a_{l'}^N| < 0.15$ and $|v_{l'}^N| < 0.23$, an improvement of 0.04 and 0.21 on previous published limits.

3.4 Gravity in extra Dimensions

The difference between the electroweak scale ($\mathrm{M}_{EW} \sim 10^2$GeV) and the scale at which quantum gravitational effects become strong, the Planck mass ($\mathrm{M}_{Pl} \sim 10^{19}$GeV), is the well known "hierarchy problem". A solution, not relying on supersymmetry or technicolour, has recently been proposed [5] that involves reducing the Planck scale to $\mathcal{O}$(TeV). This is achieved by introducing n extra submillimetre dimensions into which spin 2 gravitons propagate. The 4-dimensional Planck mass, $\mathrm{M_{Pl}}$ can be expressed in terms of the Planck scale in the $n+4$ dimensional theory, $\mathrm{M_D}$.

$$\mathrm{M_{Pl}}^2 \sim \mathrm{R^n M_D}^{\mathrm{n+2}}$$

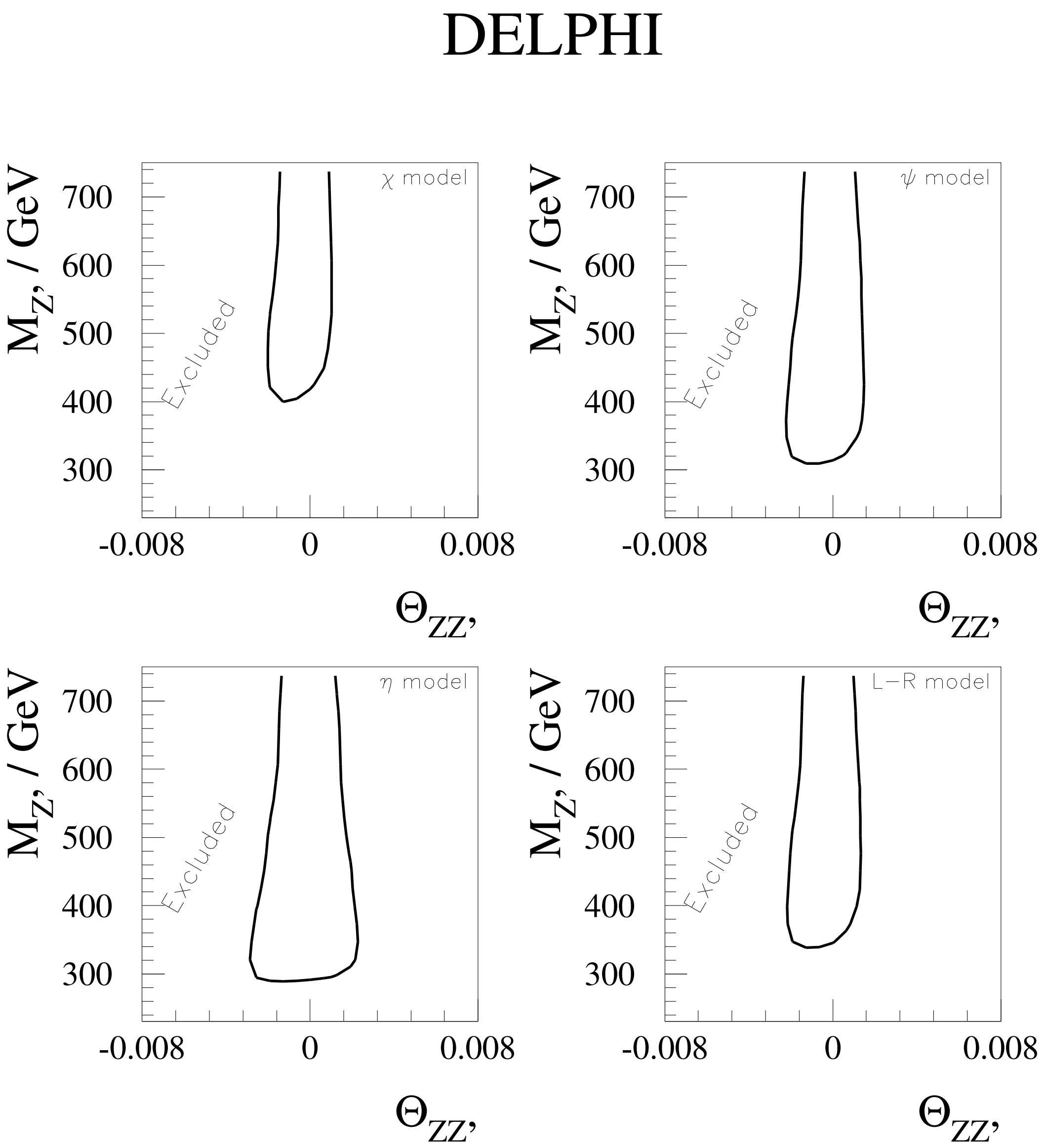

Figure 9: The allowed domain in the $M_{Z'} - \theta_{ZZ'}$ plane for the χ, ψ, η and L-R models. The contours show the 95% confidence level limits.

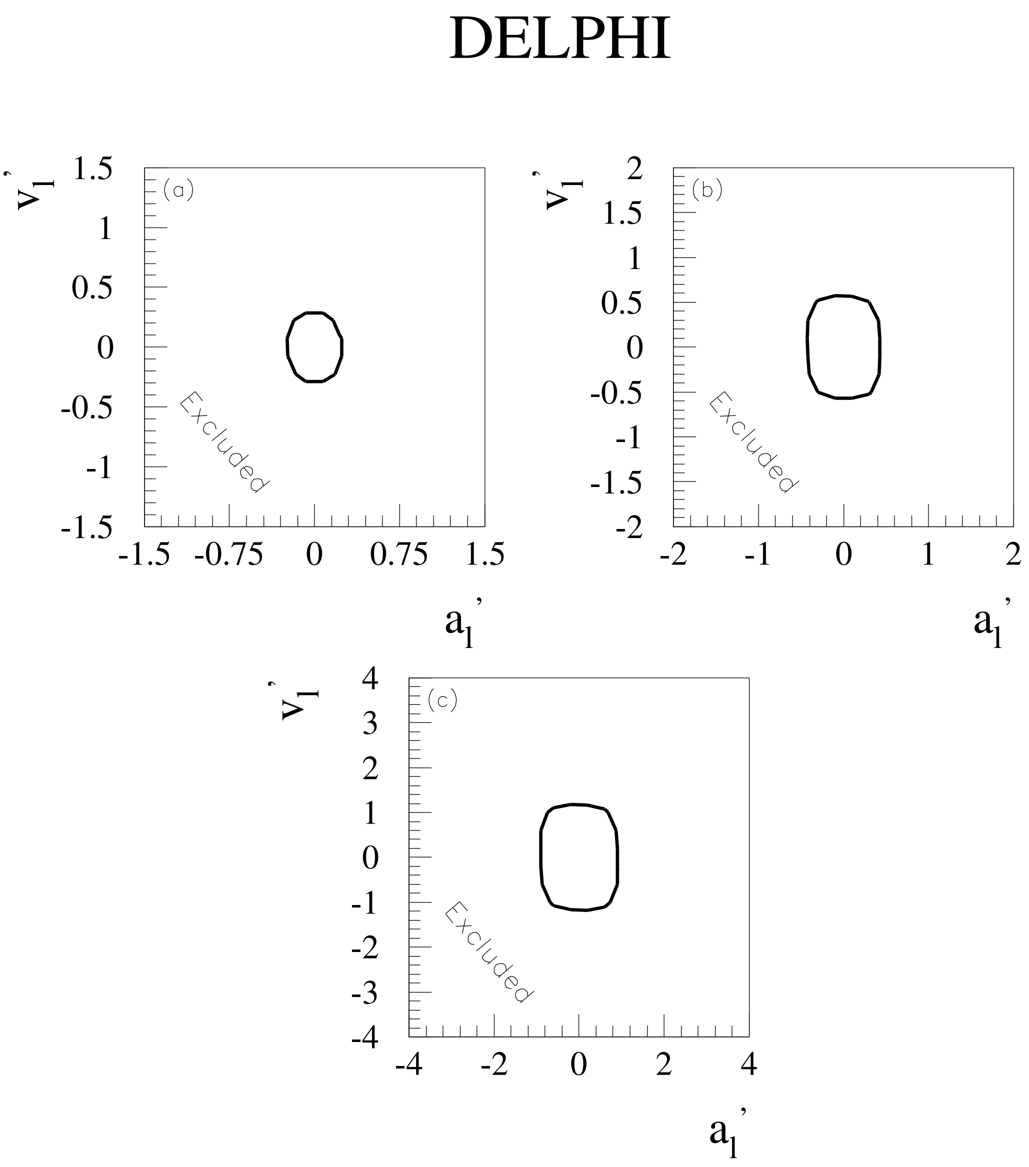

Figure 10: 95% confidence level limits on the couplings a_l' and v_l' of the Z' to leptons. The values of the Z' mass considered are 300, 500 and 1000 GeV.

where R is the size of the extra dimensions. With $\mathrm{M_D} = 1$ TeV The case where $n = 1$ is excluded as Newtonian gravitation would be modified at solar system distances whereas $n = 2$ corresponds to a radius for extra dimensions of $\sim$1mm, which is at the limit of the present sensitivity of current gravitational experiments and is therefore not excluded.

Virtual graviton exchange affects mainly the differential cross section with the largest contributions seen at low angles. Embedding the model into a string model, and identifying the Plank scale $\mathrm{M_D}$ with the string scale $\mathrm{M_s}$, the differential cross section for $e^+e^- \to f\overline{f}$ with the inclusion of the spin 2 graviton can be expressed as:

$$\frac{\mathrm{d}\sigma}{\mathrm{dz}} = A(z) + B(z)\left[\frac{\lambda}{\mathrm{M_s^4}}\right] + C(z)\left[\frac{\lambda}{\mathrm{M_s^4}}\right]^2,$$

where $z = \cos\theta$, with θ being the polar angle of production of the fermion and λ is a parameter of $\mathcal{O}(1)$. It is not possible to explicitly calculate λ without full knowledge of the underlying quantum gravitational theory, however it can be either positive or negative [6],[7].

The angular distributions were provided for non-radiative muon and tau-pairs samples at $\sqrt{s} = 189$GeV. The errors on the differential cross-sections were statistical only. A χ^2 fit for the parameter $\epsilon = \lambda/\mathrm{M_s^4}$ was performed, giving values compatible with the Standard Model, i.e. ϵ=0, and 95% lower confidence levels for the scale of extra dimensions were extracted. These limits and the best fit values are shown in Table 7. These are shown in graphical form in Figure 11 with the data and Standard Model predictions superimposed[1]. For non-physical values of ϵ, the limit is obtained using the average of the upper and lower errors on the opposite model.

4 Summary and conclusions

The results of the analysis of cross-sections and asymmetries in the channels $e^+e^- \to \mu^+\mu^-(\gamma)$, $e^+e^- \to \tau^+\tau^-(\gamma)$ and inclusive $e^+e^- \to q\bar{q}(\gamma)$, at $\sqrt{s} \sim 183 - 189$GeV were presented. The data were used to update the fits of [1] to models relying on physics beyond the Standard Model. Overall, the data agree with the Standard model predictions of ZFITTER. No evidence for physics beyond the Standard Model is found and limits were set on parameters of more general models. For instance, the scale Λ characterising contact interactions between leptons can be excluded in the range $\Lambda < 6.4 - 14.7$ TeV in several models. Alternatively Z' bosons lighter than ~ 305 GeV can be excluded at the 95% confidence level in the models considered. Lastly, lower limits on the scale $\mathrm{M_S}$ in models of gravity in extra dimensions are obtained in the region $449 - 581$ GeV for $\mu^+\mu^-$ and $\tau^+\tau^-$ final states.

Acknowledgements

We thank the SL Division of CERN for the excellent performance of the LEP collider and our funding agencies.

[1]Standard Model predictions are obtained from ZFITTERv6.11

Final State	ϵ_{Best} (TeV^{-4})	λ	$\mathrm{M_S}$(TeV)
$\mu^+\mu^-$	$-5.23^{+5.23}_{-5.56}$	-1	0.513
		$+1$	0.584
$\tau^+\tau^-$	$-12.86^{+6.67}_{-7.22}$	-1	0.449
		$+1$	0.549
l^+l^-	$-8.34^{+4.16}_{-4.36}$	-1	0.504
		$+1$	0.619

Table 7: 95% confidence level lower limits on $\mathrm{M_S}$ in models of gravity in extra dimensions for $\mu^+\mu^-$ and $\tau^+\tau^-$ final states, and for a combination of both final states, l^+l^-.

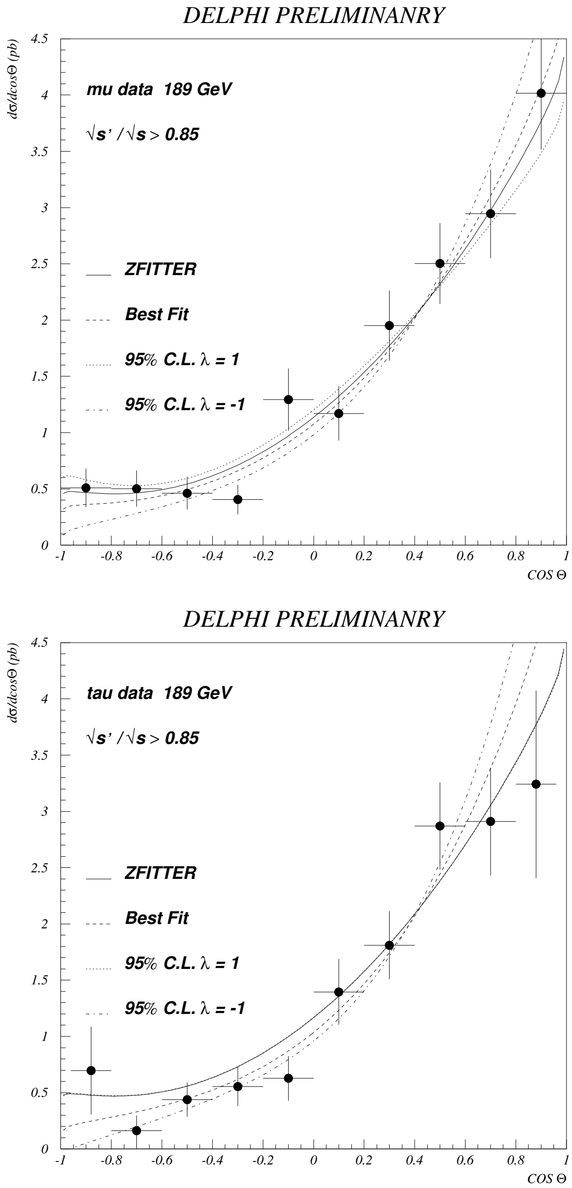

Figure 11: Fits to angular distributions for $\mu^+\mu^-$ and $\tau^+\tau^-$ final states for models which include gravity in extra dimensions.

References

[1] DELPHI Collaboration, P. Abreu *et al.* , CERN-EP 99-05

[2] DELPHI Collaboration, P. Abreu *et al.* , Nucl. Phys. **B417** (1994) 3.

[3] DELPHI Collaboration, P. Abreu *et al.* , Nucl. Phys. **B418** (1994) 403.
DELPHI Collaboration, in preparation.

[4] J. Kalinowski *et al.* , DESY 97-038.

[5] N. Arkani-Hamed *et al.* , SLAC-PUB-7864.

[6] J. L. Hewett, SLAC-PUB-8001.

[7] Gian F. Giudice *et al.* , CERN-TH/98-354.